



SCIREA Journal of Materials

<http://www.scirea.org/journal/Materials>

May 10, 2020

Volume 5, Issue 1, February 2020

# Numerical Investigation of Formation of Granular Matters Composed of Bimodal Particles

Tao Jia<sup>1,\*</sup>, Zhiyi Duan<sup>2</sup>, Bo Jia<sup>3</sup>, Di Gao<sup>4</sup>

<sup>1</sup>Department of Thermal Engineering, Taiyuan University of Technology, 030024, Taiyuan, China

<sup>2</sup>Department of Thermal Engineering, Taiyuan University of Technology, 030024, Taiyuan, China

<sup>3</sup>CITIC Pacific Mining, Perth, 6155, Australia

<sup>4</sup>Department of Mathematics and Statistics, Sam Houston State University, 1905 University Ave, Huntsville, TX 77340, United States

\* Corresponding author: Tao Jia. Email: [tjcoch@outlook.com](mailto:tjcoch@outlook.com)

## Abstract

Discrete element method is employed to numerically investigate the granular packing of frictional cohesive particles with a Bimodal distribution. In the granular particle system, the diameter of the small particle is 50 $\mu\text{m}$  and the diameter of the large particle is 100 $\mu\text{m}$ . Different particle population ratios including 2:8, 4:6, 5:5, 4:6, and 8:2 are considered. Different forces including viscoelastic force, frictional force, van der Waals force, and gravitational force are incorporated in the mathematical modeling. The effect of the friction between the colliding particles on the structure of the finally formed granular matter is studied. The values of the sliding friction coefficient are 0, 0.1, 0.2, 0.3, 0.4, and 0.5 in different cases.

It is found that the finally formed granular structure becomes looser as the sliding frictional coefficient increases. The coordination number and packing density are used to quantify the compactness of the granular structure, the characteristics of the radial distribution function and the distribution of the forces in the granular matter are investigated.

**Keyword:** granular matter; Discrete element method; Bimodal distribution; sliding friction coefficient;

## 1 Introduction

Granular matter is a special kind of matter in Nature. It shows the behaviors of dual phases including solid phase and liquid phase. It is solid-like when being packed, but it is fluid-like when flowing. The investigation of the behavior of granular matter composed of a large amount of particles has interested a lot of scientists and engineers. In nature, there are many granular matters such as sand, sugar, and salt. The unique character of granular matters is that they can flow like fluids but pack like solids. The simulation of granular particles flow based on the combination of the fluid-like and solid-like methods was carried out [1]. Granular multiphase flow was numerically investigated and the stochastic nature of the granular matter in the fluid flow was studied based on the assumption of the unilateral compressibility of the granular material [2]. An impulse-based dynamic simulation was conducted to investigate the granular flow in a hopper [3]. The crystallization phenomenon was founded in nearly jammed configurations in granular flows simulated by Discrete Element Method [4]. Discrete-element-based method [4-8] is based on the idea that if we know the behavior of each particle in a system, then we know the behavior of the whole system; the whole is the sum of the parts. The gravity-driven granular flows in which there were many interacting particles was experimentally investigated, and it was found that the interdiffusion migration caused the interaction between nonuniform particles [9]. A state of polydirectional stability was found in jammed granular matter and the stability was self-organized [10]. The ergodicity of a tapped granular system whose behavior was affected by the tapping amplitude was investigated and it was shown that there was nonergodicity under the condition of low tapping amplitude [11]. The behavior of granular matter in the process of superheating was experimentally studied and the phenomena such as spontaneous evaporation, coexistence and metastability were observed [12]. The mechanism of the agglomeration of the granular

particles is the energy dissipation during the collision of the particles. The frictional force and the viscoelastic force between the colliding particles causes the energy dissipation. The normal viscoelastic force and the tangential frictional force are often modeled based on Nonlinear Hertz theory [13] and Mindlin-Deresiewicz theory [14] respectively. Both the two theories are rooted on the idea that there is a virtual spring between the two colliding particles. As the collision occurs, the virtual spring is compressed in both the normal and the tangential directions. The normal compression is the cause of the elastic force and the tangential compression leads to the frictional force. According to Mindlin-Deresiewicz theory [14], a maximum tangential compression displacement is fixed as the normal compression deformation is known, and the friction is static friction if the tangential compression displacement is less than or equal to the maximum tangential compression displacement, the tangential compression displacement would stop increasing as soon as it reaches the maximum value; this corresponds to sliding motion in which sliding frictional force plays a role.

The difference between frictionless particles packing and frictional particles packing is that the frictionless packing is isostatic and independent of the construction history, while the frictional packing is hyperstatic and dependent on the construction history [15]. In granular gas system there are two granular temperatures including the translational granular temperature representing the translational motion of the granular particles and the rotational granular temperature representing the rotational motion of the granular particles [16]. The repose angle of the cone of a conical heap formed by pouring a lot of granular particles from a hopper onto a table was experimentally investigated, and it was shown that the repose angle depended on the surface roughness of the granular particle [17]. Based on event-driven molecular dynamics simulations, cooling process of the force-free granular gas was studied. In the simulation, the restitution coefficient is dependent on the relative impacting velocity between colliding particles [18]. The character of interstellar granular dust particles was manifested by the vibrational spectroscopy [19]. The effect of particle anisotropy on the saturated granular packing are investigated. It was found that an optimal level of anisotropy existed to make the densest packing [20]. Computational modeling is proved to be an effective way to investigate the dynamics of interstellar granular dust system because it can reveal many information that can not be obtained by observations and experiments [21].

The packing of monosized fine frictional particles was studied based on Discrete Element Method, and it was shown that the simulation can reveal the relationship between the packing

structure and the force distribution inside the packed granular matter. The relationship was difficult to be obtained by experiments due to the difficulty of experimentally measuring the forces between the particles [22].

The above research works all focus on the granular packing of monosized particles packing. We have investigated granular packing of the particles with Gaussian distribution, and we studied the effect of the frictional coefficient on the packing structure [23]. The present paper studies the granular packing of particles with Bimodal size distribution. The packing geometric structure of the granular matter is quantified by porosity, coordination number, and radial distribution function, and the distributions of the forces inside the granular matter composed of Bimodal-sized particles are investigated.

## 2 Mathematical Model and Numerical Simulation

Newtonian mechanics is employed to describe the motion of each particle in the granular system. The translational and rotational movements of the particle are described by Eq.(1) and Eq.(2) respectively.

$$m_i \frac{d^2 \mathbf{r}_i}{dt^2} = \mathbf{F}_i = \sum_j (\mathbf{F}_{ij}^n + \mathbf{F}_{ij}^t + \mathbf{F}_{ij}^v) + m_i \mathbf{g} \quad (1)$$

$$I_i \frac{d\boldsymbol{\omega}_i}{dt} = \mathbf{T}_i = \sum_j (\mathbf{T}_{ij}^t + \mathbf{T}_{ij}^r) \quad (2)$$

where  $m_i$  is the mass of the particle,  $\mathbf{r}_i$  the position of the particle,  $\boldsymbol{\omega}_i$  the angular velocity of the particle,  $I_i$  the inertial moment of the particle.  $\mathbf{F}_i$  the resultant force exerting on the particle, and  $\mathbf{T}_i$  the torque acting on the particle. The subscripts  $ij$  indicates acting on the particle  $i$  by particle  $j$ , where  $\mathbf{F}_{ij}^n$  and  $\mathbf{F}_{ij}^t$  are the normal contact force and the tangential frictional force respectively,  $\mathbf{F}_{ij}^v$  the van der Waals force which actually always exists no matter how apart two particles are,  $\mathbf{T}_{ij}^t$  the torque caused by the tangential contact force, and  $\mathbf{T}_{ij}^r$  the torque caused by the rolling frictional force.

According to nonlinear Hertz theory [13], the normal contact force on particle  $i$  is calculated as:

$$\mathbf{F}_{ij}^n = \left[ \frac{2}{3} E \sqrt{\bar{R}} \xi_n^{3/2} - \gamma E \sqrt{\bar{R}} \sqrt{\xi_n} (\mathbf{v}_{ij} \cdot \mathbf{n}_{ij}) \right] \mathbf{n}_{ij} \quad (3)$$

where  $Y$  is Young's modulus and  $\sigma$  Poisson's ratio,  $E = Y / (1 - \sigma^2)$ ,  $\bar{R}$  is the effective radius calculated as  $\bar{R} = R_i R_j / (R_i + R_j)$  in which  $\mathbf{R}_i$  and  $\mathbf{R}_j$  are the position vectors. The direction of the vector  $\mathbf{R}_i$  is pointing to the contact point between particle  $i$  and particle  $j$  from the center of particle  $i$ . Similarly the direction of the vector  $\mathbf{R}_j$  is pointing to the contact point between particle  $i$  and particle  $j$  from the center of particle  $j$ ,  $\gamma$  is the damping coefficient,  $\mathbf{v}_{ij}$  is the velocity of particle  $i$  relative to particle  $j$ ,  $\xi_n = R_i + R_j - |R_{ij}|$  is the deformation between the two particles,  $R_{ij}$  is the distance between the centers of particle  $i$  and the center of particle  $j$ , and  $\mathbf{n}_{ij}$  is the unit vector pointing to the center of particle  $i$  from the center of particle  $j$ .

Based on Mindlin-Deresiewicz theory [14], the frictional force in the tangential is determined as:

$$\mathbf{F}_{ij}^t = \mu |\mathbf{F}_{ij}^n| \left[ 1 - \left( 1 - \frac{|\xi_t|}{|\xi_{\max}|} \right)^{1.5} \right] \mathbf{t}_{ij} \quad (4)$$

where  $|\mathbf{F}_{ij}^n|$  is the absolute value of the normal contact force between the two colliding particles : particle  $i$  and particle  $j$ ,  $\mu$  is the sliding friction coefficient between the two colliding particles,  $\xi_t = \int_{t_0}^t \mathbf{v}_t dt$ , it is the tangential displacement which is integrated from the starting time of the contact between the two colliding time to the time when the tangential displacement stops increasing.  $\mathbf{v}_t$  is the relative velocity in the tangential direction at the contact point where particles  $i$  and particles  $j$  meet. It is calculated as the following:

$$\mathbf{v}_t = (\mathbf{v}_i - \mathbf{v}_j) \cdot \mathbf{t}_{ij} + (\boldsymbol{\omega}_i \times \mathbf{R}_i - \boldsymbol{\omega}_j \times \mathbf{R}_j) \quad (5)$$

where  $\boldsymbol{\omega}_i$  and  $\boldsymbol{\omega}_j$  are angular velocities of particles  $i$  and  $j$  respectively,  $\mathbf{t}_{ij}$  is the unit vector in tangential direction. In the simulation, according to Mindlin-Deresiewicz theory [14], the tangential displacement  $\xi_t$  is set as  $\xi_{\max}$ , if  $\xi_t$  is larger than  $\xi_{\max}$  which is the maximum tangential displacement  $\xi_{\max}$  and is calculated as the following:

$$\xi_{\max} = \mu \frac{2-\sigma}{2-2\sigma} \xi_n \quad (6)$$

As the particle size comes to micrometer scale, the van der Waals force comes to play a role and it is determined as:

$$\mathbf{F}_{ij}^v = -\frac{H_a}{6} \times \frac{64R_i^3 R_j^3 (h + R_i + R_j)}{(h^2 + 2R_i h + 2R_j h)^2 (h^2 + 2R_i h + 2R_j h + 4R_i R_j)^2} \mathbf{n}_{ij} \quad (7)$$

where  $H_a$  is Hamaker constant which depends on the material of the particle, and  $h$  is the distance between the fronts of particle  $i$  and particle  $j$ .

The above is the introduction of the forces involved in the simulation. Now the torque acting on the particle needs to be investigated. There are two types of torques including the torque caused by the tangential contact force and the torque caused by the rolling frictional force.

The torque caused by the tangential contact force is denoted as  $\mathbf{T}_{ij}^t$  which is calculated as:

$$\mathbf{T}_{ij}^t = \mathbf{R}_i \times \mathbf{F}_{ij}^t \quad (8)$$

The torque acting on particle  $i$  by particle  $j$  due to the rolling frictional force between the two particles is the following:

$$\mathbf{T}_{ij}^r = -\mu_r R_i \left| \mathbf{F}_{ij}^n \right| \boldsymbol{\omega}_i \quad (9)$$

where  $\mu_r$  is the coefficient of the rolling friction between the two particles. Verlet method [23-25] is employed to solve eq. (1) and (2).

At the beginning stage of the simulation, 3375(15×15×15) particles are put in a rectangular box. This arrangement is that there are 15 layers in each coordinate direction in the three-dimensional Cartesian system. At the boundaries in the horizontal directions periodical boundary condition is applied. The particle diameter value can only be two distinct values: 50μm or 100μm. Regarding the property of the granular particle, the sliding frictional coefficient  $\mu$  takes six distinct values: 0( this corresponds to the situation of absolutely smooth particle), 0.1, 0.2, 0.3, 0.4, and 0.5, the mass density is 2500 kg / m<sup>3</sup>, Young's modulus  $Y$  is 10<sup>7</sup> N / m<sup>2</sup>, Poisson's ratio  $\sigma$  is 0.3, rolling frictional coefficient  $\mu_r$  is 0.002, the damping coefficient  $\gamma$  is 2.0×10<sup>-5</sup> s, and Hamaker constant  $H_a$  is 6.5×10<sup>-20</sup> J.

### 3 Result and discussion

The finally formed granular matters composed of Bimodal particles are shown in Figure 1. In this case the sliding frictional coefficient is 0.3. The configurations of the granular matters in the cases of other sliding frictional coefficients are similar. So we do not plot them here.

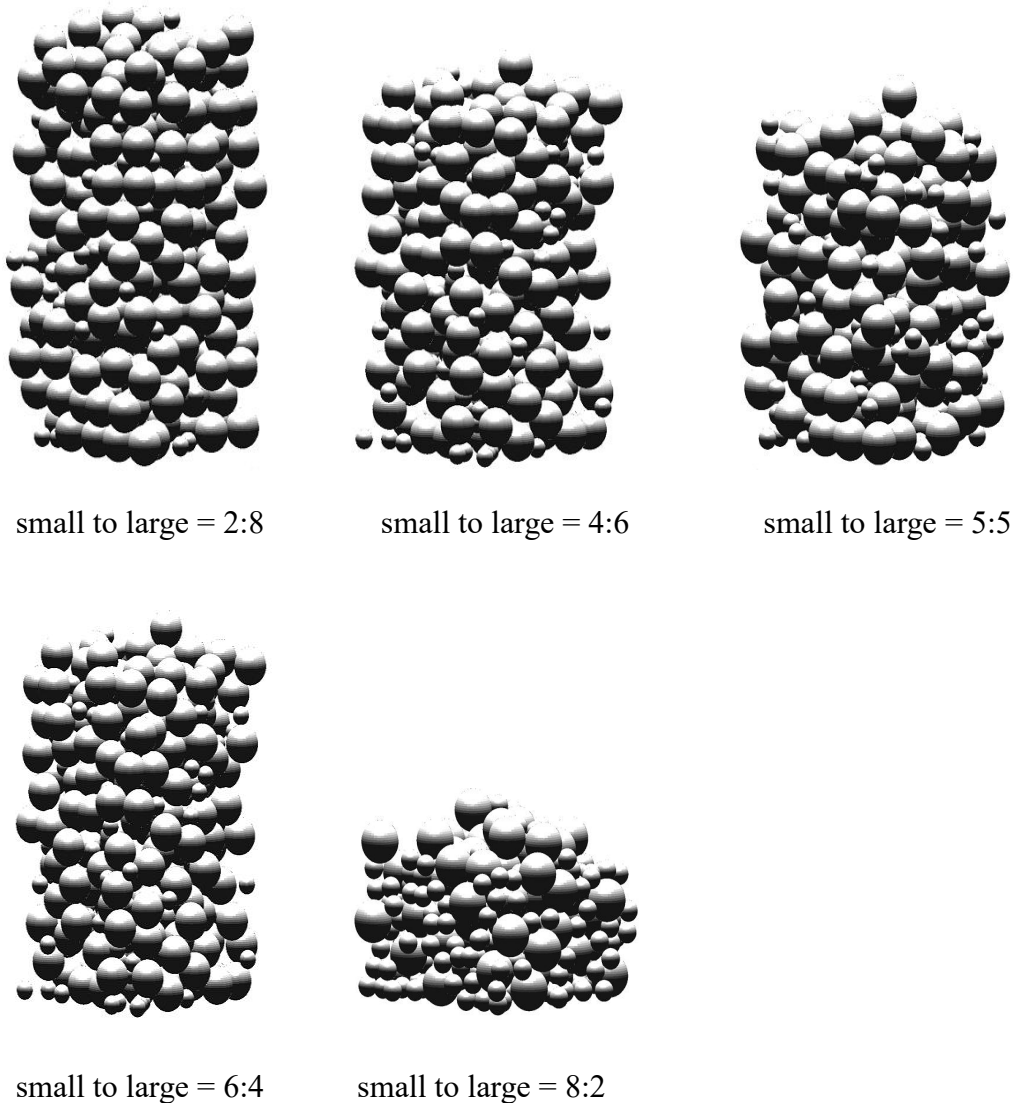


**Figure 1** Configurations of granular matters formed under the conditions of different particle population ratios.

#### 3.1 Coordination number and packing density

Coordination number and packing density are used to qualitatively measure the

compactness of the granular matter. In the granular matter, the coordination number of one particle is the number of particles touching it. The average coordination number is the average value of the coordination numbers of all particles. Packing density is fraction of the space filled by the granular matter.

It is shown in Figure 2 and Figure 3 that the coordination number and the packing density all decrease with the increase of the sliding frictional coefficient. This means that the increase of the sliding frictional coefficient loosens the structure of the granular matter. This is same under the condition of particles with Gaussian distribution [23].

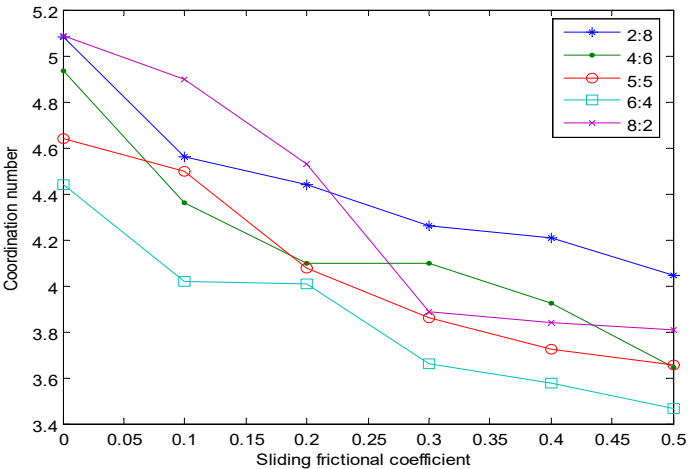


**Figure 2 The change of coordination number with sliding frictional coefficient**

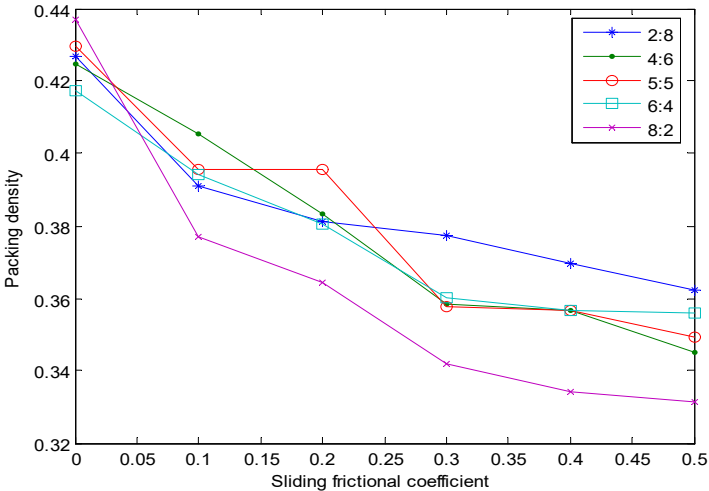


**Figure 3 The change of packing density with sliding frictional coefficient**

### 3.2 Radial distribution function

To measure the probability of finding a granular particle at a place with a certain distance from a reference point, Radial distribution function is commonly used. It is mathematically defined as the following:

$$g(r) = \frac{dN(r)}{4\pi r^2 dr \rho} \quad (10)$$

where  $\rho$  is the number density of particles; the number of particles in unit space.  $N(r)$  is the particle number in a spherical space with radius  $r$ .

Figure 4 shows the radial distribution functions of the Bimodal granular particles in a granular matter formed under the conditions of different particle population ratios (small to large). The sliding frictional coefficient is 0.3. Since the radial distribution functions in the cases of other sliding frictional coefficients are similar when plotted, we do not present them here. The radius of the small particle is set as the unit of the distance  $r$ . The RDF functions have three peak values at  $r = 2, 3, 4$ . The number 2 corresponds to the case of the contact between two small particles. The number 3 corresponds to the case of the contact between a small particle and a large particle.

The number 4 corresponds to the case of the contact between two large particles.

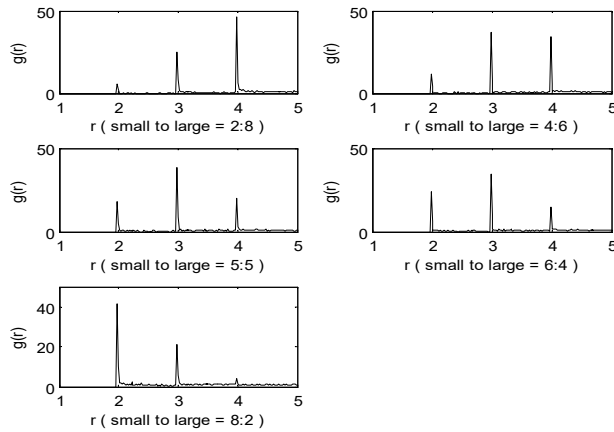


**Figure 4 Radiation distribution functions of the packing structures with different particle population ratio**

### 3.3 Force distribution inside granular matter

For a spherical particle inside the granular matter, it is acted by contact force, van der Waals

force, and gravitational force. The contact force is the resultant force of the normal viscoelastic force and the tangential frictional force. Van der Waals force and gravitational force are all long-range force. No matter how far apart the two particles are, van der Waals force and gravitational force all exist. The difference between the two forces is that gravitational force is always downward, while van der Waals force has no favorite direction; it is randomly distributed inside the granular matter.

To calculate the distribution of the contact force and the van der Waals force inside the granular matter, we first calculate the contact force and the van der Waals force acting on every particle, and then the forces are scaled by the gravitational force acting on the particle, as shown in Eq(11) and (12):

$$z_i^c = \left| \sum_j \mathbf{F}_{ij}^c \right| / |m_i \mathbf{g}| \quad (11)$$

$$z_i^v = \left| \sum_j \mathbf{F}_{ij}^v \right| / |m_i \mathbf{g}| \quad (12)$$

where  $z_i^c$  is the ratio of the magnitude of the all contact forces acting on particle  $i$  to the magnitude of the gravitational force acting on particle  $i$ , and  $z_i^v$  is the ratio of the magnitude of the all van der Waals forces acting on particle  $i$  to the magnitude of the gravitational force acting on particle  $i$ .  $z_i^c$  and  $z_i^v$  are named nondimensionalized contact force and nondimensionalized van der Waals force respectively here.

It can be seen from Figure 5 and Figure 6 that the probability distributions of the contact force and the van der Waals force are different. The probability distribution of the contact force shows exponential tail-like pattern, and the nondimensionalized contact force mainly focuses between 0 and 100. As to the probability distribution of the van der Waals force, it shows bell-shape-like pattern when the nondimensionalized van der Waals force is between 0 and 2, and it has discrete peak values when the nondimensionalized van der Waals force is between 2 and 5. This is different from situation of Gaussian particles packing in which the probability distribution of the van der Waals force inside granular matter shows bell-shape-like pattern when the nondimensionalized van der Waals force is between 0 and 4, and decreases to zero when it is larger than 4 [23].

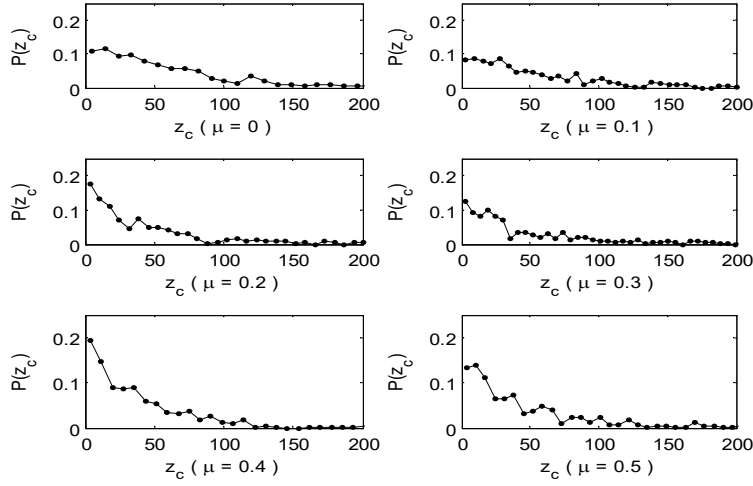


**Figure 5** The distribution of contact force inside the granular matter

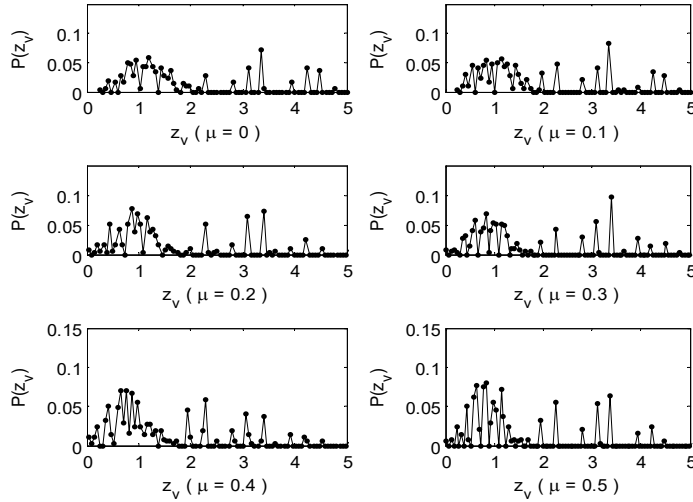


**Figure 6** The distribution of van der waals force inside the granular matter

As to the probability distribution of the contact force shown in Figure 5, the equation (13) works well to describe the trend of the data obtained from the simulation.

$$P(z_c) = a \cdot e^{-b \cdot z_c} \quad (13)$$

where  $z_c$  is the nondimensionalized contact force,  $P(z_c)$  is the probability of the nondimensionalized contact force,  $a$  and  $b$  are two constants. Equation(13) describes a tail-like curve. The larger is the parameter  $a$ , the steeper is the curve, and the larger is the parameter  $b$ , the flatter is the curve. The different values of the parameters  $a$  and  $b$  under different conditions of particle population ratio and sliding frictional coefficient are listed in

Table 1. It can be seen in Table 1 that the smallest value of parameters  $a$  and the largest value of parameters  $b$  occurs under the situation where the sliding frictional coefficient is 0.5 and the population ratio of small particle to large particle is 8:2.

For the probability distribution of the van der Waals force, the equation (14) fits the data when the nondimensionalized van der Waals force is between 0 and 2. As mentioned before this is different from the result of granular packing of particles with Gaussian size distribution [23] where the probability decreases to zero when the value of the nondimensionalized van der Waals force is larger than 2. In the current case of the bimodal particles packing, when the nondimensionalized van der Waals force is larger than 2, the probability still has some discrete peak values. The probability decreases to zeros when the nondimensionalized van der Waals force is larger than 5.

$$P(z_v) = I \cdot e^{-(z_v-c)^2/(2\sigma^2)} \quad (14)$$

where  $z_v$  is the nondimensionalized van der Waals force,  $P(z_v)$  is the probability of the nondimensionalized van der Waals force,  $I$ ,  $c$ , and  $\sigma$  are three constants. The different values of  $I$ ,  $c$ , and  $\sigma$  under different conditions of particle population ratio and sliding frictional coefficient are listed in Table 2. The largest value of  $\sigma$  occurs under the condition where the sliding frictional coefficient is 0 and the population ratio of small particle to large particle is 8:2. The value of  $\sigma$  determines the width of the bell-shape like curve described by the equation (14), the larger is  $\sigma$ , the wider range is the distribution. The physical meaning of the parameter  $c$  is that the bell-shape like curve described by the equation (14) is symmetric around  $z_v = c$ . Under the condition of the constant sliding frictional coefficient, the value of  $c$  shows a general increasing trend as the population ratio of small particle to large particle increases.

**Table 1 Parameters in the formula (13) describing contact force distribution**

Particle Population ratio (small particle to large particle)	$\mu = 0$	$\mu = 0.1$	$\mu = 0.2$	$\mu = 0.3$	$\mu = 0.4$	$\mu = 0.5$
--	-----------	-------------	-------------	-------------	-------------	-------------

2:8	a=0.14 b=0.015	a=0.195 b=0.018	a=0.195 b=0.024	a=0.195 b=0.026	a=0.1 b=0.02	a=0.22 b=0.024
4:6	a=0.14 b=0.016	a=0.09 b=0.014	a=0.18 b=0.025	a=0.125 b=0.025	a=0.2 b=0.025	a=0.16 b=0.025
5:5	a=0.08 b=0.014	a=0.16 b=0.017	a=0.105 b=0.026	a=0.14 b=0.022	a=0.14 b=0.028	a=0.15 b=0.028
6:4	a=0.09 b=0.026	a=0.10 b=0.026	a=0.10 b=0.028	a=0.11 b=0.028	a=0.16 b=0.028	a=0.16 b=0.034
8:2	a=0.05 b=0.015	a=0.06 b=0.02	a=0.10 b=0.022	a=0.07 b=0.022	a=0.14 b=0.026	a=0.05 b=0.038

**Table 2 Parameters in the formula (14) describing van der Waals force distribution**

Particle Population ratio (small particle to large particle)	$\mu = 0$	$\mu = 0.1$	$\mu = 0.2$	$\mu = 0.3$	$\mu = 0.4$	$\mu = 0.5$
2:8	$I = 0.09$ $c = 1$ $\sigma = 0.25$	$I = 0.08$ $c = 1$ $\sigma = 0.25$	$I = 0.12$ $c = 0.7$ $\sigma = 0.22$	$I = 0.13$ $c = 0.75$ $\sigma = 0.22$	$I = 0.1$ $c = 0.75$ $\sigma = 0.24$	$I = 0.14$ $c = 0.75$ $\sigma = 0.22$
4:6	$I = 0.06$ $c = 1$ $\sigma = 0.26$	$I = 0.055$ $c = 1$ $\sigma = 0.28$	$I = 0.08$ $c = 0.8$ $\sigma = 0.28$	$I = 0.07$ $c = 0.8$ $\sigma = 0.28$	$I = 0.07$ $c = 0.75$ $\sigma = 0.26$	$I = 0.08$ $c = 0.75$ $\sigma = 0.26$

5:5	$I = 0.045$ $c = 1.3$ $\sigma = 0.34$	$I = 0.06$ $c = 1$ $\sigma = 0.32$	$I = 0.075$ $c = 1$ $\sigma = 0.24$	$I = 0.05$ $c = 0.75$ $\sigma = 0.24$	$I = 0.05$ $c = 0.75$ $\sigma = 0.26$	$I = 0.06$ $c = 0.75$ $\sigma = 0.26$
6:4	$I = 0.05$ $c = 1.25$ $\sigma = 0.26$	$I = 0.052$ $c = 1$ $\sigma = 0.25$	$I = 0.055$ $c = 1.25$ $\sigma = 0.26$	$I = 0.05$ $c = 1$ $\sigma = 0.26$	$I = 0.075$ $c = 1$ $\sigma = 0.23$	$I = 0.06$ $c = 0.8$ $\sigma = 0.22$
8:2	$I = 0.04$ $c = 1.5$ $\sigma = 0.34$	$I = 0.055$ $c = 1.5$ $\sigma = 0.30$	$I = 0.06$ $c = 1.5$ $\sigma = 0.31$	$I = 0.08$ $c = 1.5$ $\sigma = 0.30$	$I = 0.06$ $c = 1.5$ $\sigma = 0.30$	$I = 0.05$ $c = 1$ $\sigma = 0.3$

## 4 Conclusions

Discrete element method is employed to study the agglomeration of fine particles with Bimodal size distribution. The agglomerations under the conditions of different are investigated. The dissipative forces including viscoelastic and frictional forces act as the cause of the agglomeration. It is found that the packing structure becomes less compact as the sliding frictional coefficient increases. Both coordination number and packing density are used to describe the compactness. To describe the change of the particle number density with the change of the distance from a reference particle, radial distribution functions are calculated. This reveals the different types inter-particle contacts including the contact between large particle, the contact between small particles, and the contact between large particles and small particles inside the granular matters. The probability distribution of the contact force exhibits tail-like character and the probability distribution of the van der Waals force shows bell-shape-like character.

## References

- [1] Eslamian, A., Khayat, M.: A novel hybrid solid-like fluid-like (SLFL) method for the simulation of dry granular flows, *Particuology*, **31**, 200–219 (2017)
- [2] Ku, K.S., An, C.H., Li, Kim, K.C., M.I.: An Eulerian model for the motion of granular material with a large Stokes number in fluid flow, *International Journal of Multiphase Flow*, **92**, 140–149 (2017)
- [3] Toson, P., Khinast, J. G.: Impulse-based dynamics for studying quasi-static granular flows: Application to hopper emptying of non-spherical particles, *Powder Technology*, **313**, 353–360 (2017)
- [4] Khalilitehrani, M., Sasic, S., Rasmuson, A.: Multiscale rheophysics of nearly jammed granular flows in a high shear system, *Powder Technology*, **315**, 356–366 (2017)
- [5] Marra, F. S., Troiano, M., Montagnaroc, F., Salatino, P., Solimene, R.: Particle–wall interaction in entrained-flow slagging coal gasifiers: Granular flow simulation and experiments in a cold flow model reactor, *International Journal of Multiphase Flow*, **91**, 142–154 (2017)
- [6] Cundall, P. A., Strack, O. D. L.: A discrete numerical model for granular assemblies, *Geotechnique*, **29**, 47-65(1979)
- [7] Sykut, J., Molenda, M., Horabik, J.: DEM simulation of the packing structure and wall load in a 2-dimensional silo, *Granular Matter*, **10**, 273-278(2008)
- [8] Mobius, R., Heussinger, C.: (Ir)reversibility in dense granular systems driven by oscillating forces, *Soft Matter*, **10**, 4806–4812(2014)
- [9] Dolgunin, V.N., Kudi, A.N., Ukolov, A.A., Tuev, M.A.: Rapid granular flows on a vibrated rough chute: Behaviour patterns and interaction effects of particles, *Chemical Engineering Research and Design*, **122**, 22–32 (2017)
- [10] Zimmer, F., Kollmer, J.E., Poschel, T.: Polydirectional Stability of Granular Matter, *Physical Review Letters*, **111**, 168003, (2013)
- [11] Paillusson, F., Frenkel, D.: Probing Ergodicity in Granular Matter, *Physical Review Letters*, **109**, 208001 (2012)
- [12] Pacheco-Vázquez, F., Caballero-Robledo, G. A., Ruiz-Suares, J. C.: Superheating in Granular Matter, *Physical Review Letters*, **102**, 170601 (2009)

- [13] Dintawa, E., Tijsskens, E.: Ramon, H.: On the accuracy of the Hertz model to describe the normal contact of soft elastic spheres, *Granular Matter*, **10**, 209-221(2008)
- [14] Mindlin, R.D., Deresiewicz, H.: Elastic spheres in contact under varying oblique forces, *Journal of Applied Mechanics*, **20**, 327-344(1957)
- [15] Leonardo, E. S., Deniz, E., Gary, S. G., Thomas, C. H., Dov, L.: Geometry of frictionless and frictional sphere packings, *Physical Review E*, **65**, 041304, (2003)
- [16] Zippelius, A.: Granular gases, *Physica A*, **369**, 143–158 (2006)
- [17] Herrmann, H.J.: Granular matter, *Physica A*, **313**, 188 – 210 (2002)
- [18] Bodrova, A., Chechkin, A. V., Cherstvy, A. G., Metzler, R.: Quantifying non-ergodic dynamics of force-free granular gases, *Physical Chemistry Chemical Physics*, **17**, 21791 -21798 (2015)
- [19] Herbst, E.: Three milieux for interstellar chemistry: gas, dust, and ice, *Physical Chemistry Chemical Physics*, **16**, 3344-3359 (2014)
- [20] Cieřla, M., Pajk, G., Ziff, R.M.: Shapes for maximal coverage for two-dimensional random sequential adsorption, *Physical Chemistry Chemical Physics*, **17**, 24376 (2015)
- [21] Bromley, S. T., Goumans, T. P. M., Herbst, E., Jones, A. P., Slater, B.: Challenges in modelling the reaction chemistry of interstellar dust, *Physical Chemistry Chemical Physics*, **16**, 18623-18643 (2014)
- [22] Yang, R. Y., Zou, R. P., Yu, A. B.: Computer simulation of the packing of fine particles, *Physical Review E*, **62**, 3900-3907, (2000)
- [23] Jia, T., Gao, D.: Simulation of granular packing of frictional cohesive particles with Gaussian size distribution, *Applied Physics A*, **12**, 8031-8037, 2016
- [24] Rapaport, D. C.: *The Art of Molecular Dynamics Simulation* (Cambridge University Press, Cambridge, 1995)
- [25] Haile, J. M.: *Molecular Dynamics Simulation: Elementary Method* (John Wiley & Sons, Inc, 1992)